

Mycelium-Enhanced Bacterial Degradation of Organic Pollutants under Bioavailability Restrictions

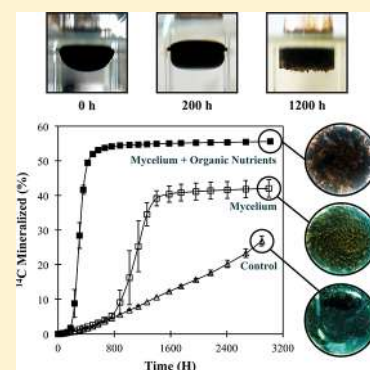
Rungroch Sunthong,^{†,||} Margalida Tauler,[‡] Magdalena Grifoll,[‡] and Jose Julio Ortega-Calvo^{*,†,||} 

[†]Instituto de Recursos Naturales y Agrobiología de Sevilla (IRNAS-CSIC), Avenida Reina Mercedes 10, Seville 41012, Spain

[‡]Department of Genetics, Microbiology and Statistics, Faculty of Biology, University of Barcelona, Diagonal 643, Barcelona 08028, Spain

 Supporting Information

ABSTRACT: This work examines the role of mycelia in enhancing the degradation by attached bacteria of organic pollutants that have poor bioavailability. Two oomycetes, *Pythium oligandrum* and *Pythium aphanidermatum*, were selected as producers of mycelial networks, while *Mycobacterium gilvum* VM552 served as a model polycyclic aromatic hydrocarbon (PAH) degrading bacterium. The experiments consisted of bacterial cultures exposed to a nondisturbed nonaqueous phase liquid (NAPL) layer containing a heavy fuel spiked with ¹⁴C-labeled phenanthrene that were incubated in the presence or absence of the mycelia of the oomycetes in both shaking and static conditions. At the end of the incubation, the changes in the total alkane and PAH contents in the NAPL residue were quantified. The results revealed that with shaking and the absence of mycelia, the strain VM552 grew by utilizing the bulk of alkanes and PAHs in the fuel; however, biofilm formation was incipient and phenanthrene was mineralized following zero-order kinetics, due to bioavailability limitations. The addition of mycelia favored biofilm formation and dramatically enhanced the mineralization of phenanthrene, up to 30 times greater than the rate without mycelia, possibly by providing a physical support to bacterial colonization and by supplying nutrients at the NAPL/water interface. The results in the static condition were very different because the bacterial strain alone degraded phenanthrene with sigmoidal kinetics but could not degrade alkanes or the bulk of PAHs. We suggest that bacteria/oomycete interactions should be considered not only in the design of new inoculants in bioremediation but also in biodegradation assessments of chemicals present in natural environments.



INTRODUCTION

Hydrophobic organic pollutants (e.g., polycyclic aromatic hydrocarbons (PAHs)), due to their low aqueous concentrations, often exhibit low bioavailability, which limits the metabolic activities and affects the community structures of pollutant-degrading microorganisms.^{1–8} Examples of chemicals with restricted bioavailability include PAHs sorbed to natural organic matter and associated with nonaqueous phase liquids (NAPLs), e.g., crude oil and lubricants, matrices in which these chemicals show a reduced chemical activity.^{4–7} Recent attempts to enhance the bioavailability and biodegradation of PAHs provided new insights into low-risk ecological approaches to optimizing bioremediation.⁶ One approach is the exploitation of natural chemical enhancers (e.g., biosurfactants and plant root exudates) to accelerate the partitioning rate of PAHs from NAPLs or boost the tactic responses of PAH-degrading bacteria toward distant pollutant sources.^{2–4,7–9} Additionally, improvements in pollutant bioavailability using mycelial networks formed by eukaryotic microbes (e.g., fungi and oomycetes) have recently been proposed as promising biological enhancers for facilitating the transport of PAH-degrading bacteria and PAHs, leading to increased rates of biodegradation.^{10–13}

Two conceptual applications of mycelial networks are considered in the bioremediation of PAH-polluted scenar-

ios.^{10–15} First, the mycelial networks provide thin liquid films of water as routes that induce self-propelled PAH-degrading bacteria to perform tactic responses toward PAHs. Second, the extended hyphae within the growing mycelial networks provide linked cytoplasmic channels as the routes for pollutant transport. Although increasing PAH bioavailability is an established role of mycelial networks in ecologically adapted bioremediation, the optimum application of mycelial networks remains uncertain. For example, how can mycelial networks promote the transport and metabolic activities of nonpropelled PAH-degrading bacteria? Hence, the examination of the dynamics of PAHs in low bioavailability scenarios and the presence of mycelia would demonstrate what functions and mechanisms by which mycelia could perform and impact metabolic activities of PAH-degrading bacteria.

Recently, our studies revealed that the motile offspring, so-called “zoospores,” produced from mycelial networks of the oomycete *Pythium aphanidermatum* mobilized both non- and self-propelled PAH-degrading bacteria and formed microbial

Received: June 22, 2017

Revised: September 12, 2017

Accepted: September 18, 2017

Published: September 18, 2017

consortia at NAPL/water interfaces.^{16,17} Such microbial consortia are initiated by the settlement of zoospores at the interfaces between NAPLs and water, which is followed by germination and the formation of mycelial networks by zoospore cysts onto and into the NAPLs. This sequential phenomenon is likely the initiation of complex biofilms that can enhance PAH bioavailability and sustain the growth of PAH-degrading bacteria.^{18–20} However, the structures and roles of biofilms formed at the NAPL/water interface remain poorly known, particularly those of PAH-degrading bacteria and mycelial networks. Further evaluations of the interactive links between these biofilms and the biodegradation of restricted bioavailable PAHs could therefore provide an optimal implementation of such microbial consortia in bioremediation.

With the aim of elucidating the ecological applications of mycelial networks in the bioremediation of low-bioavailable pollutants, we established a model pollution scenario in which PAHs were in a biphasic NAPL/water system prepared with a heavy fuel oil/alkane mixture. The system allows a low chemical activity of the PAHs due to their association to the NAPL, thus restricting their bioavailability, and it maintains the integrity of the organic phase and hence a constant interfacial area.⁷ The bacterium *Mycobacterium gilvum* VM552 was selected as a nonpropelled pollutant-degrader, and two oomycetes, *Pythium oligandrum* and *P. aphanidermatum*, were used as the producers of mycelial networks. The experiments were constructed in a biometer system under shaken and static conditions, and the dynamics of phenanthrene as a model PAH was tracked with isotope labeling. At the end of the incubation, the changes in the total alkane and PAH contents in the NAPL residue were quantified. The links between the interfacial biofilms of the microbial cocultures and the PAH-degrading activities of the bacterium are discussed in this study.

MATERIALS AND METHODS

Chemicals. PAHs, phenanthrene-9-¹⁴C (13.1 mCi mmol⁻¹, radiochemical purity >98%), 2,2,4,4,6,8,8-heptamethylnonane (HMN), and 17 α (H),21 β (H)-hopane were purchased from Sigma-Aldrich, Germany. Heavy fuel oil RMG 35 (ISO 8217) was obtained from the Technical Office of Accidental Marine Spills, University of Vigo, Spain.⁷

Microbial Strains, Cultivation, and Preparation. *M. gilvum* VM552 (a PAH-degrading bacterium) was supplied by D. Springael (Catholic University of Leuven, Belgium). This bacterium can utilize various PAHs and alkanes as carbon and energy sources. The bacterial strain was preserved in 20% (v/v) glycerol at -80 °C. The bacterium was grown on tryptic soy agar (Sigma-Aldrich, Germany) at 30 °C for 4–7 days and then transferred to a mineral salt medium supplemented with 0.02 g mL⁻¹ of phenanthrene as the sole source of carbon and energy.⁷ The inoculated culture broth was incubated at 30 °C with shaking at 150 rpm. When the culture reached the exponential phase of growth (~96 h of incubation), the excess phenanthrene was removed by filtration through a glass fiber filter (pore size, $\varnothing = 40 \mu\text{m}$). The culture filtrate was then incubated overnight under the same growing conditions described above for complete phenanthrene removal by biodegradation. Bacterial cells were collected by centrifugation at 4303g, washed twice, and resuspended in sterilized lake water (by autoclaving at 121 °C for 15 min). This natural lake water was collected at Embalse Torre del Águila, Seville, Spain, and kept frozen (-80 °C) until use. The lake water is an optimal solution for oomycete development and has a low concen-

tration of dissolved organic carbon (9 mg L⁻¹), as well as traces of phosphorus (P) and nitrogen (N).¹⁶ Bacterial cell density was adjusted at 600 nm absorbance (OD_{600 nm}) to 1 (corresponding to ~10⁸ colony forming units or CFU mL⁻¹), which was used further as an inoculum for mineralization experiments.

Two oomycetes, *P. oligandrum* and *P. aphanidermatum*, were used in this study. *P. oligandrum* CBS 530.74 (a mycoparasitic oomycete used as a biocontrol agent against pathogenic fungi and oomycetes) was purchased from Centraalbureau voor Schimmelcultures (CBS), Fungal Biodiversity Centre, Institute of the Royal Netherlands Academy of Arts and Sciences, Utrecht, The Netherlands. *P. aphanidermatum* (a massive zoospore-producing oomycete) was supplied by the Aberdeen Oomycete Laboratory, University of Aberdeen, UK. Both oomycetes are able to form mycelia (filamentous growth) on solid agar medium and to produce biflagellate zoospores under certain conditions (e.g., submerged and aqueous environments). However, we did not observe zoospores produced by *P. oligandrum* under the same conditions used for zoospore formation of *P. aphanidermatum*. The two oomycetes were grown routinely on diluted V8 (DV8) agar medium following the protocol described elsewhere.¹⁶ DV8 agar medium contains V8 juice (Campbell Soup Company, UK). According to the analysis of a sample performed in our laboratory, this medium has 548 mg L⁻¹ of total organic carbon, 820 mg L⁻¹ of total N and 157 mg L⁻¹ of total P. Although both oomycetes form mycelia on this agar medium, the density of biomass (mycelia) per area of growth ($\mu\text{g cm}^{-2}$) was different. *P. aphanidermatum* could form 2-times denser mycelia than *P. oligandrum* (data not shown). Two different forms of mycelia were prepared as the inocula for the mineralization experiments, including solely mycelia (no DV8 agar medium) and mycelia growing on DV8 agar medium (mycelia + DV8). After growing each oomycete on DV8 agar medium for 4 days, the seeded agar medium was cut into pieces of 1 cm². The inoculum with solely mycelia was prepared after removing DV8 agar medium by scraping aerial mycelia from the medium surfaces, while mycelia-growing agar pieces served as the inoculum of mycelia + DV8. A total of 20 pieces of either mycelia or mycelia + DV8 was introduced in an individual mineralization assay.

Mineralization Experiments and Rate Determination.

The experiments were performed using a biometer flask that contained a trap (1 mL of 0.5 M NaOH) for CO₂ and an open-end glass cylinder ($\varnothing = 2 \text{ cm}$, 10 cm length, and four 2 mm slots in the base) to maintain the physical integrity of the NAPL/water interface, as described elsewhere.⁷ Sterilized lake water (70 mL) was introduced into the flask and mixed with 1 mL of bacterial suspension to give a final concentration of approximately 10⁷ CFU mL⁻¹. The flask was then supplemented with 1) 20 pieces of oomycete mycelia (solely mycelia), 2) 20 pieces of mycelia-growing DV8 agar medium (mycelia + DV8), or 3) 20 pieces of DV8 agar medium (solely DV8). The control flasks had only the bacterial suspension or only the mycelia-growing DV8 agar medium of each oomycete (20 pieces in total as well). Within the prepared biometer flasks, 1 mL of NAPL was added to the open-end glass cylinder fixed at the center of the flask. The NAPL was a mixture of heavy fuel oil with HMN at a 1:1 ratio (w/v) to reduce the fuel viscosity. The radiolabeled ¹⁴C-phenanthrene was added to the NAPL at an approximate final concentration of 50 000 dpm mL⁻¹, and the solution was homogenized by shaking at 150 rpm for a few hours. The cylinder base allowed the circulation of the medium

from outside, and prevented the contact of the agar pieces with the NAPL/water interface.

The mineralization experiments were performed at least in duplicate and incubated at 25 °C either aerated by shaking reciprocally at 80 rpm or in a static condition. One mL of NaOH added in the biometer flasks was continuously collected and replaced with new one along the mineralization experiments until the mineralization curves reached the plateau phases (approximately 125 days for shaken conditions and up to 190 days for static conditions). The $^{14}\text{CO}_2$ -trapped NaOH was measured for its radioactivity after mixing with scintillation cocktail by using an LS 6500 Scintillation Counter (BECKMAN COULTER, USA). The mineralization activity of *M. gilvum* VM552 was estimated by the production of $^{14}\text{CO}_2$. No significant loss of $^{14}\text{CO}_2$ was expected during the mineralization experiments because all biometer flasks were sealed with Teflon-lined closures. This closed biometer flask system was verified for $^{14}\text{CO}_2$ losses in previous work with soils and showed the complete recovery of nonmineralized ^{14}C residues by combustion of the solids in a biological oxidizer.²¹ The mineralization rate of phenanthrene by strain VM552 was calculated using at least five successive points derived from the mineralization curve of the ^{14}C mineralized versus incubation time. The five successive points were selected from the slope of each mineralization curve, approximately at mid log phase for the sigmoid curve and approximately at midphase for the straight-line curve. The initial mass of phenanthrene in 1 mL of NAPL was 210 μg ; 1 dpm of ^{14}C -labeled phenanthrene corresponded to 4.2 ng of the total phenanthrene.

End-Point Mass Balance of ^{14}C and Characterization of NAPL Residues. At the end of the mineralization experiments, the NAPL residues were gently removed from biometer flasks, and all the remaining solids were separated from the aqueous phase by centrifugation at 4303g for 10 min. The solids were resuspended in a known volume of distilled water and dispersed roughly with a spatula. The suspension was then sonicated for 1 h in a sonicator bath (Branson 3510) and homogenized with a vortex for a few min. The radioactivity in the solid and the aqueous phase was determined with the scintillation counter. The percentage of ^{14}C remaining in the NAPL was calculated by the difference between the total ^{14}C recovered and the initial ^{14}C . The direct measurement of this fraction was not possible because of inflammability and quenching caused by the fuel present in the samples.

The collected NAPL residues were subsequently analyzed for their hydrocarbon composition. Each NAPL sample was dissolved in dichloromethane, dried over Na_2SO_4 , and concentrated to 5 mL. The saturated and aromatic hydrocarbon fractions were then separated by column chromatography following US-EPA method 3611b and analyzed by GC-MS as described elsewhere.²² The degradation percentages of the fuel total alkanes and of US-EPA PAHs and alkyl derivatives were determined by comparing the hopane-normalized areas from reconstructed ion chromatograms to those obtained from controls. The alkanes were determined using m/z 85 as a diagnostic ion, while PAHs and their alkyl derivatives were detected using their corresponding molecular ions.²³ 17 α -(H),21 β -(H)-Hopane was used as the conserved internal marker (ion m/z 191). The alkane HMN was not analyzed because it was used as a nondegradable component of the NAPL.^{7,16}

To evaluate the effect of biofilms formed at the NAPL/water interfaces on the mineralization activities of *M. gilvum* VM552,

we observed the macroscopic changes in biofilm growth and NAPL hydrophobicity during the mineralization experiments. The NAPL/water interfaces were screened for biofilm growth by direct observation, and the detected biofilms were photographed at the end of the mineralization experiments. The microscopic structures of the interfacial biofilms were also photographed after staining with 0.02% (v/v) acridine orange and visualizing with a fluorescence microscope (Axioskop 2 Carl Zeiss, Jena, Germany). The NAPL hydrophobicity was determined by measuring the contact angle (θ_{nw}) after perpendicular photography of the buoyant NAPL fixed in the glass cylinder at the center of each biometer flask. With the aim of discriminating the impacts of growth and development of oomycetes on the levels of dissolved oxygen (DO) and dissolved organic carbon (DOC) that would cause some influence on the bacterial degradation, we also measured these parameters. A set of experiments imitating the mineralization experiments was carried out, using an oxygen meter (OXI 45 DL, CRISON) for DO and a Shimadzu TOC-VCSH with ASI-V auto sampler after filtration through Whatman No. 1 (pore size, $\varnothing = 11 \mu\text{m}$) for DOC.

Statistical Analyses. The mean value \pm standard deviation (SD) or standard error (SE) derived from any measurement is reported. Comparison of multiple means was performed by appropriate analysis of variance (ANOVA) with Tukey's *post hoc* test in the SPSS 21.0 program (SPSS, Chicago, IL, USA). The statistical results are reported with the *F*-distribution, degrees of freedom and significant (*P*) value.

RESULTS AND DISCUSSION

Enhancement of Pollutant Biodegradation by Mycelia. The effects of *P. oligandrum* and *P. aphanidermatum* mycelia on the bacterial mineralization of phenanthrene initially present in the NAPL are shown in Figure 1 and Supporting Information (SI) Figure S1, respectively. Under shaking conditions (Figure 1a), *M. gilvum* VM552 mineralized phenanthrene at a slow rate and following zero-order kinetics. The mineralization curves in the presence of *M. gilvum* VM552 and the oomycetes were S shaped (logistic kinetics). When the oomycetes growing on DV8 agar were supplied, the bacterial metabolism occurred at significantly higher rates than in the presence of the bacterium only (Table 1). *P. oligandrum* caused a greater enhancement of the bacterial mineralization of phenanthrene than *P. aphanidermatum*. Such a difference in the enhancement caused by distinct oomycete species suggested that the effect was highly dependent upon the growth and development of oomycetes. The control supplemented with DV8 agar alone showed a stimulatory effect on *M. gilvum* VM552, but the maximum mineralization rates were significantly higher when the oomycetes were also present. The other controls containing only the oomycetes growing on DV8 agar resulted in negligible rates of mineralization of phenanthrene (lower than 0.01 $\text{ng mL}^{-1} \text{h}^{-1}$), which confirmed that the bacterium was solely responsible for the transformation.

In our previous work, static conditions were identified as favorable for oomycete growth and development in a set of PAH-polluted scenarios.^{16,17} Therefore, we conducted a set of mineralization experiments in which the flasks were allowed to stand without further shaking. The static conditions resulted in two contrasting effects on phenanthrene mineralization. First, *M. gilvum* VM552 alone mineralized phenanthrene following logistic kinetics (Figure 1b) with a maximum rate that was

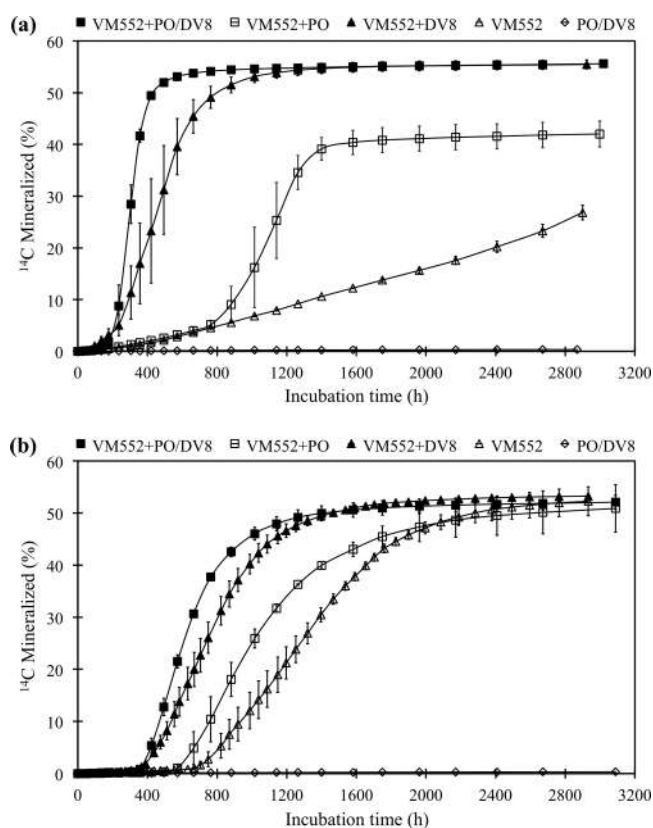


Figure 1. Effect of *Pythium oligandrum* mycelia on bacterial mineralization of ^{14}C -phenanthrene initially associated with the nonaqueous phase liquid (NAPL). The experiments were conducted under shaking (a) and static (b) conditions. The treatments included *Mycobacterium gilvum* VM552 plus *P. oligandrum* growing on DV8 agar (VM552+PO/DV8), *M. gilvum* VM552 plus *P. oligandrum* mycelia (VM552+PO), *M. gilvum* VM552 plus DV8 agar (VM552+DV8), *M. gilvum* VM552 alone as a positive control (VM552), and *P. oligandrum* growing on DV8 agar as a negative control (PO/DV8). Error bars represent the standard error from at least duplicate experiments.

significantly higher than the rate under shaking conditions (Table 1). Second, the static conditions led to a significantly lower rate of phenanthrene mineralization in the treatment with *M. gilvum* VM552 and the oomycetes growing on DV8 agar than the shaking conditions (Table 1). However, the rate remained significantly higher than the static controls with the

bacterium only, with and without DV8 agar. Thus, under static conditions, the mycelia enhanced the transformation.

The relatively high extents of phenanthrene mineralization observed (Table 1) were consistent with the nearly complete consumption of the chemical initially present in the NAPL as demonstrated by GC-MS analysis of the phenanthrene remaining in the NAPL at the end of incubation (Table 2). The analysis showed that the losses of phenanthrene were higher than 95% in all treatments except for the shaken cultures containing only the bacterium. The differences in the extent of mineralization between these treatments (Table 1) could be explained by the incorporation of different proportions of substrate carbon into microbial biomass or transformed to partially oxidized byproducts, which is a characteristic of growth-linked biodegradation.²¹ Therefore, the distribution of the nonmineralized phenanthrene carbon was determined (Table 2). Despite the nearly complete phenanthrene disappearance, the results indicated that a significantly high percentage of ^{14}C remained associated with the NAPL at the end of incubation (up to 35.21% in the treatment with *P. oligandrum* mycelia under shaking conditions (Table 2)). Very low percentages of ^{14}C (0.32–2.42%) were detected in the aqueous and solid fractions of the treatments that contained the oomycete growing on DV8 agar (Table 2). These findings are consistent with the negligible metabolism of phenanthrene by the oomycete, as well as the low sorption of the chemical to the oomycete biomass.

The strain *M. gilvum* VM552 was selected for this study because of its capacity to mineralize phenanthrene, but this bacterium can also degrade other PAHs and alkyl derivatives in addition to alkanes present in the fuel. The degradation pattern by *M. gilvum* VM552 of the different components of this fuel mixture is described elsewhere.⁷ In this study, the GC-MS analysis of the NAPL residues at the end of incubation showed the biodegradation of the primary components in the NAPL, including both aromatic and aliphatic hydrocarbons, under shaking conditions (SI Table S1 and Figures S2 and S3). The treatment containing only *P. oligandrum* exhibited the typical profile of the nondegraded fuel and was therefore chosen as the reference for the other treatments.⁷ Co-inoculation with the oomycete mycelia and the addition of DV8 had no effect on the final extent of the biodegradation of total PAHs and alkanes under shaking conditions. However, very limited bacterial degradation of the bulk of the fuel components was observed under static conditions (SI Table S1). The selective degradation of phenanthrene (Table 2) was consistent with

Table 1. Effect of Oomycete Mycelia on Bacterial Mineralization of ^{14}C -Phenanthrene Initially Present in the Nonaqueous Phase Liquid^a

| treatment | inoculum | DV8 agar ^b | maximum mineralization rate ($\text{ng mL}^{-1} \text{h}^{-1}$) | | mineralization extent (%) | |
|--|----------|-----------------------|---|---------------|---------------------------|-------------|
| | | | shaken | static | shaken | static |
| <i>Mycobacterium gilvum</i> VM552 | – | – | 0.29 ± 0.04a | 1.31 ± 0.09a* | 26.8 ± 2.0a | 53.2 ± 5.9* |
| | + | – | 3.24 ± 0.07b | 2.10 ± 0.10b* | 55.5 ± 1.5c | 53.4 ± 0.2 |
| <i>M. gilvum</i> VM552 + <i>Pythium oligandrum</i> | – | – | 2.03 ± 0.16ab | 1.72 ± 0.22ab | 42.0 ± 4.3b | 51.3 ± 6.7* |
| | + | – | 8.27 ± 1.21d | 2.90 ± 0.28c* | 55.6 ± 1.3c | 52.2 ± 2.4 |
| <i>M. gilvum</i> VM552 + <i>Pythium aphanidermatum</i> | – | – | 1.67 ± 0.23ab | 1.75 ± 0.14ab | 28.9 ± 0.2a | 48.9 ± 0.3* |
| | + | – | 5.86 ± 1.39c | 2.72 ± 0.35c* | 49.6 ± 5.7bc | 53.3 ± 0.7 |

^aThe results are reported as the mean ± SD derived from duplicate or triplicate experiments. ^bThe treatments contained (+) or did not contain (–) diluted V8 (DV8) agar (see text for details). Values in each column followed by the same lowercase letter are not significantly different according to a one-way ANOVA at $P = 0.05$. Asterisks indicate that the means under static conditions are significantly different from the corresponding values under shaking conditions based on two-way ANOVA and simple main effects tests at $P = 0.05$.

Table 2. Effect of *Pythium oligandrum* Mycelia on Depletion of Phenanthrene Initially Present in the NAPL and Phase Distribution of Nonmineralized $^{14}\text{C}^a$

| inoculum | treatment | DV8 agar ^b | phenanthrene remaining in NAPL (%) ^c | | | | | | nonmineralized ^{14}C (%) | | | | | | | |
|---|-----------|-----------------------|---|----------------------|-------------|---------------|--------------|--------------|------------------------------------|---------------|----------------------|----------------------|---------------|--------------|---------------|---------------|
| | | | shaken | | static | | shaken | | shaken | | static | | shaken | | static | |
| | | | shaken | static | shaken | static | shaken | static | shaken | static | shaken | static | shaken | static | shaken | static |
| <i>Mycobacterium gilvum</i> VM552 | - | - | 28.4 ± 7.4b | 3.19 ± 1.36a* | 53.1 ± 4.3c | 23.0 ± 1.2c* | 14.9 ± 4.2b | 17.9 ± 1.8bc | 4.53 ± 0.04ab | 5.87 ± 2.29b | 18.8 ± 2.3a | 14.3 ± 2.2ab* | 17.9 ± 2.8b | 18.8 ± 1.8bc | 7.90 ± 2.64bc | 13.4 ± 1.0c* |
| | | | 0.92 ± 0.09a | 2.27 ± 0.49a | 18.8 ± 2.3a | 14.3 ± 2.2ab* | 17.9 ± 2.8b | 17.9 ± 2.8b | 18.8 ± 1.8bc | 7.90 ± 2.64bc | 13.4 ± 1.0c* | 17.9 ± 2.8b | 14.3 ± 2.2ab* | 17.9 ± 2.8b | 18.8 ± 1.8bc | 7.90 ± 2.64bc |
| <i>M. gilvum</i> VM552 + <i>P. oligandrum</i> | - | - | 1.09 ± 0.21a | 2.73 ± 0.05a | 35.2 ± 2.2b | 8.7 ± 4.2a* | 16.5 ± 1.2b | 22.5 ± 2.4c* | 6.27 ± 1.07bc | 17.5 ± 1.8d* | 0.89 ± 0.26a | 3.25 ± 0.93a | 17.4 ± 1.3b | 16.9 ± 2.2b | 10.27 ± 0.73c | 11.3 ± 0.8c |
| | | | 0.89 ± 0.26a | 3.25 ± 0.93a | 16.7 ± 0.6a | 19.6 ± 1.8bc | 17.4 ± 1.3b | 17.4 ± 1.3b | 16.9 ± 2.2b | 10.27 ± 0.73c | 11.3 ± 0.8c | 17.4 ± 1.3b | 19.6 ± 1.8bc | 17.4 ± 1.3b | 16.9 ± 2.2b | 10.27 ± 0.73c |
| <i>P. oligandrum</i> | + | + | control ^d | control ^d | 96.7 ± 0.5d | 97.9 ± 0.5d | 2.42 ± 0.46a | 1.33 ± 0.22a | 0.50 ± 0.01a | 0.40 ± 0.30a | control ^d | control ^d | 96.7 ± 0.5d | 97.9 ± 0.5d | 0.50 ± 0.01a | 0.40 ± 0.30a |

^aThe results are reported as the mean percentage ± SD derived from duplicate or triplicate experiments, which were measured at the end of the mineralization experiments. ^bThe treatments contained (+) or did not contain (-) diluted V8 (DV8) agar (see text for details). ^cThe results are derived from GC-MS analysis. ^dNondegraded NAPL chosen as the reference for other treatments. Values in each column followed by the same lowercase letter are not significantly different, supported by separate one-way ANOVA at $P = 0.05$. Asterisks indicate that the means under the static conditions are significantly different from the corresponding values under the shaking conditions based on two-way ANOVA and simple main effects tests at $P = 0.05$.

the fact that the strain had been pregrown with this substrate as the sole carbon source (the phenanthrene-degrading enzymes were present) and its very low concentration compared with that of the other individual fuel components (4.3% of total PAHs).

Roles of Mycelia in Promoting Bacterial Colonization at the NAPL/Water Interface. The NAPL in contact with the microbial suspension formed a stable interface between this hydrophobic layer and the water, where the phase exchange of chemicals took place. Our results in Tables 1 and 2 indicated that the mycelia enhanced the biodegradation of phenanthrene through the stimulation of microbial colonization of the NAPL/water interface. In the absence of mycelia and under shaking conditions, the mineralization of phenanthrene occurred linearly at a constant rate that was very similar to the partitioning rate of the chemical (0.2 ng mL⁻¹ h⁻¹) measured under the same conditions (i.e., NAPL/water interface area and shaking speed) in a previous study from our group, what indicates bioavailability restrictions.⁷ However, mycelia enhanced the mineralization rates of phenanthrene by the bacterium, which exceeded those of the partitioning rate predictions (Table 1). Logistic, partitioning uncoupled kinetics can be observed during the biodegradation of organic chemicals in NAPLs, when the microorganisms proliferate attached to the NAPL/water interfaces, where they acquire directly the chemicals.^{4,7,24} The significant presence of nonmineralized phenanthrene C in the NAPL at the end of the experimental period, when phenanthrene had disappeared (Table 2), could be attributed to the attached bacterial cells that had assimilated the chemical.

The morphology of the NAPL/water interface was observed during the mineralization experiments to determine if physical changes at the NAPL/water interface, induced by the mycelia, were linked to bacterial degradation. In side view, the NAPL displayed a convex shape at the start of the experiments, which gradually changed during the incubation (Figure 2a). The changes in the NAPL side views corresponded to the evolution of the NAPL/water contact angle (θ_{nw}), which was associated with the NAPL hydrophobicity. The θ_{nw} value was approximately 120° at the start of the experiments and gradually decreased during the experimental period. Such macroscopic changes were attributed to a reduction of the NAPL hydrophobicity, which were observed in most treatments regardless the different conditions tested and were associated with the kinetics of phenanthrene mineralization (Table 1 and Figure 1). Under shaking conditions, the change of the NAPL/water contact angle was more rapid when mycelia were present, which was consistent with the onset in the mineralization rates (Figure 1a). The unchanged θ_{nw} value of the controls without the bacterium corresponded with the negligible biodegradation of the NAPL components (including phenanthrene) in addition to the absence of apparent growth of the oomycetes (Table 1). These findings indicated that in addition to wettability and contact time,^{25,26} microbial communities dwelling at the NAPL/water interface also have a significant effect on the NAPL hydrophobicity.

The interfacial biofilms were macroscopically observed at the end of the mineralization experiments, and the biofilms were relatively denser in the treatments with oomycete mycelia (Figure 2b). Such abundant biofilms were relevant to the apparent macroscopic changes of the fuel layer, as reflected by the evolution of θ_{nw} . The aspect of the biofilms was also different depending upon the treatment. For example, in

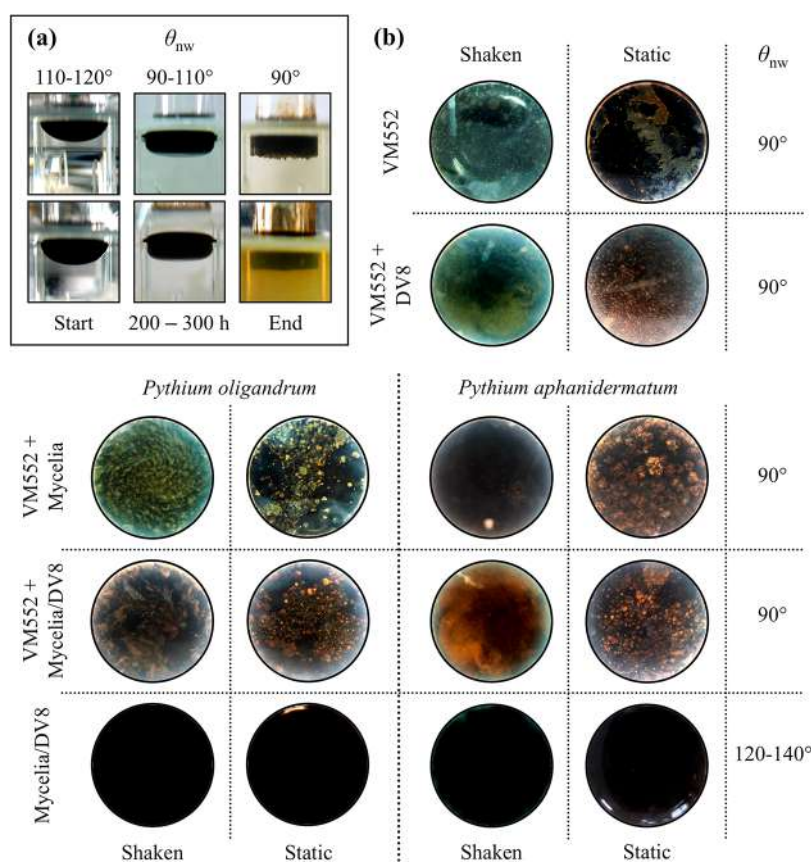


Figure 2. Effects of microbial growth on the morphological evolution of NAPL and macroscopic structures of microbial biofilms colonized at NAPL/water interfaces. The morphological evolution of NAPL determined with the change of contact angle (θ_{nw}) was visualized along the mineralization experiments (a). The macroscopic structures of microbial colonization in form of biofilms at NAPL/water interfaces were photographed at the end of incubation (b). All photographs present in part a were derived from the experiments under shaken (top) and static (bottom) conditions that contained *Mycobacterium gilvum* VM552 and *Pythium oligandrum* growing on diluted V8 (DV8) agar. The photographs present in part b refer to all treatments indicated in Figure 1 and SI Figure S1. The diameters of these photographs correspond to the inner diameters of the glass cylinders (2 cm).

shaking conditions, the pattern of colonization in the treatment with only *M. gilvum* VM552 cells was characterized by discrete colonies randomly formed throughout the fuel surface, while in those treatments with mycelial supplements, a swirl pattern developed as a result of reciprocal shaking (Figure 2b). We confirmed by epifluorescence microscopy, the presence of both microbial components (*M. gilvum* VM552 cells and oomycete mycelium) in the biofilms formed at the NAPL/water interfaces.

The mechanism by which oomycetes facilitated biofilm formation at the NAPL/water interface could be based on a biophysical effect. The colonization of the interface by mycelia possibly occurred through the filamentous growth and/or the release of reproductive propagules (e.g., hyphal fragments, oospores and zoospores), what formed mycelial networks at the interface.^{12,16,24} Such networks can provide paths for bacterial transport to reach and colonize the NAPL/water interface, which is a well-known mechanism, called the “fungal highway effect”, for enhancing pollutant bioavailability and biodegradation.^{11–15} This biophysical facilitation was observed with the hydrophilic mycelia of *Pythium ultimum*,¹³ which belongs to the same phylogenetic cluster of both oomycete species used in this work. Also, *Mycobacterium* spp. can perform surface motility on moist or wet surfaces, although their cells are hydrophobic and nonflagellated.^{12,27} The floating mycelia might play some role in moderating the Brownian motion of bacterial cells by

reducing the shear forces within the aqueous microenvironments caused by shaking. It is also possible that oomycetes release zoospores that have a tactic response to diverse substrata (including pollutant/water interfaces) at the remote microhabitats in which they settle and initiate sibling mycelial networks.^{16,17,28} Indeed, oomycete zoospores are able to mobilize directionally *M. gilvum* VM552 cells under a steady-flow environment.¹⁷ Moreover, *P. aphanidermatum* zoospores exhibited selective settlement and formed hyphae penetrating a single-component NAPL (hexadecane),¹⁶ which is relevant to this study as hexadecane is also an alkane component of heavy fuel oil (SI Figure S2).

It is also possible that the growth and development of the oomycetes at the NAPL/water interface provided an exchange platform for essential metabolites and elements. In this context, the logistic kinetics observed with DV8 medium was consistent with this nutritional effect at the NAPL/water interface. The selective biodegradation of phenanthrene under static conditions that occurred in the absence of mycelia and DV8 medium can also be understood because under these conditions, the diffusion of oxygen also limited bacterial metabolism and biosynthesis at the interface. The higher percentages of phenanthrene degradation than those of the bulk of the PAHs corresponded to the relatively low concentration of phenanthrene in the fuel and the preference of the strain for this substrate under such conditions. In fact,

the inoculated *M. gilvum* VM552 cells were pregrown on phenanthrene and could readily and selectively mineralize this compound. According to this mechanism, attached bacteria mineralized phenanthrene under static conditions at an even higher rate than under shaking conditions (i.e., even when partitioning of the chemical was expected to be slower, relying on diffusion only), because the simultaneous consumption of the other NAPL components, with the subsequent competition effects, did not occur. This made the stimulation by the oomycetes (and the DV8 medium) less evident. Alternately, it is also possible that, under static conditions, more *M. gilvum* VM552 cells could have accumulated at the interface, resulting in a faster phenanthrene mineralization. However, this explanation is unlikely because it is not consistent with the preferential phenanthrene biodegradation observed in static conditions (i.e., the other NAPL components were not degraded at a higher extent).

Roles of Dissolved Oxygen and Dissolved Organic Carbon. Because the growth and development of oomycetes could modify the concentration of dissolved oxygen (DO), which would have an effect on the biodegradation of hydrocarbons (particularly under static conditions), the concentrations of DO were measured. The measurements were performed in the absence of NAPL and bacterial inoculum, to prevent any interference from, respectively, NAPL toxicity and bacterial consumption of DO, but the rest of the conditions were kept the same as for the mineralization experiments (SI Figure S4). The DO levels always remained at approximately 6 mg L⁻¹ during the experimental period of 700 h, regardless of whether the biometer flasks were inoculated with the oomycetes or incubated under shaking or static conditions. The growth of oomycetes was also confirmed macroscopically at the end of the assay. The levels of DO revealed the concentration of DO was not limiting for bacterial degradation. The concentrations of DO detected in this study are much higher than the half-saturation coefficient for DO ($K_{DO} = 0.094$ mg L⁻¹) that *Mycobacterium* requires to reach the maximum growth rate in the presence of a single PAH.²⁹ Also, a DO concentration as low as 0.034 mg L⁻¹ has no influence on alkane biodegradation in sediment microcosms.²⁹

A possible role of mycelia in the production of dissolved organic carbon (DOC), which could have enhanced the biodegradation of hydrocarbons by increasing their partitioning rates from the NAPL to the aqueous phase, driven by sorption to dissolved macromolecules,^{8,30} was also examined. The concentration of DOC was determined in assays that simulated the conditions during the mineralization experiments but without the NAPL and the bacterium (SI Figure S5). Without any oomycete inoculum and under both shaking and static conditions, the DV8 agar blocks passively released DOC to reach an equilibrium concentration of 150 mg L⁻¹ after 480 h of the incubation. The equilibrium concentration of DOC was significantly lower when the assays were inoculated with the oomycete growing on DV8 agar (100 mg L⁻¹) and with the oomycete mycelia only (20 mg L⁻¹). No significant effect was detected between the shaking and static conditions on the variation of DOC concentration. In theory, these low DOC concentrations were not sufficient to cause an enhancement in the net partitioning of phenanthrene into the aqueous phase, which would explain the mineralization rates in this study. Taking into account a DOC concentration of 150 mg L⁻¹ in the aqueous phase and the log K_{oc} of phenanthrene, which is 4.16,¹⁶ the predicted total concentration of the compound in

the aqueous phase (and the resulting net partitioning rate, assuming instantaneous equilibrium with DOC)^{8,30} was only enhanced 3-fold, which is significantly lower than the 10-fold enhancement observed (Table 1). However, assuming a general figure of 1 pg C per microbial cell,²¹ the complete transformation into bacterial cells of the DOC released from the DV8 agar would have caused a 15-fold increase of the bacterial population initially present (10⁷ cells mL⁻¹). It is possible, therefore, that the DV8 agar contributed to increase the density of suspended bacteria, which eventually attached to the NAPL/water interface, thus promoting its colonization.

In summary, the data show that mycelia enhanced the bacterial degradation of hydrophobic organic pollutants under the bioavailability restrictions imposed by a NAPL. Promoting bacterial colonization at the pollutant/water interfaces through a biophysical effect, by facilitating the translocation of bacteria through the radial expansion of mycelial growth and release of productive propagules, and providing an exchange platform for metabolites and minerals at the interface, are proposed here as the possible mechanisms for the enhancement of pollutant bioavailability and biodegradation. The exact mechanisms operating under static conditions, that may be representative of some environments, such as soil, will be the subject for further research. Nevertheless, this study provides new insights into the role of bacteria/oomycete interactions in the colonization of interfaces, which is important for designing new inoculants in bioremediation. The results have also implications for studies focused on the persistence of chemicals in natural environments, by highlighting the possible influence of mycelia on the activity of pollutant-degrading bacterial communities that develop at the surfaces of NAPLs and aggregates in soils and sediments.

■ ASSOCIATED CONTENT

📄 Supporting Information

The Supporting Information is available free of charge on the ACS Publications website at DOI: 10.1021/acs.est.7b03183.

Table S1: Effect of *Pythium oligandrum* on bacterial degradation (%) of total PAHs and alkanes initially present in the nonaqueous phase liquid. Figure S1: Effect of *Pythium aphanidermatum* mycelium on bacterial mineralization of ¹⁴C-phenanthrene initially associated with the NAPL. Figure S2: Effect of *Pythium oligandrum* on the hopane-normalized areas (A/A_{Hop}) of PAHs and alkyl-PAHs analyzed by molecular ions based GC-MS. Figure S3: Effect of *Pythium oligandrum* on the hopane-normalized areas (A/A_{Hop}) of *n*-alkanes analyzed by *m/z* 85-based GC-MS. Figure S4: Evolution of dissolved oxygen (DO) concentration in the aqueous phase of mineralization experiments. Figure S5: Evolution of dissolved organic carbon (DOC) concentration in the aqueous phase of mineralization experiments (PDF)

■ AUTHOR INFORMATION

Corresponding Author

*Phone: (+34) 954 624 711. Fax: (+34) 954 624 002. E-mail: jjortega@imase.csic.es.

ORCID

Jose Julio Ortega-Calvo: 0000-0003-1672-5199

Present Address

^{||}R.S.: Infrastructure and Environmental Research Division, School of Engineering, University of Glasgow, Glasgow G12 8LT, UK.

Notes

The authors declare no competing financial interest.

ACKNOWLEDGMENTS

We thank the Spanish Ministry of Science and Innovation (CGL2010-22068-C02-01, CGL2013-44554-R, and CGL2016-77497-R), the Andalusian Government (RNM 2337), the European Commission (LIFE15 ENV/IT/000396), and the CSIC JAE Program (RS) for funding support.

REFERENCES

- (1) Chen, B.; Wang, Y.; Hu, D. Biosorption and biodegradation of polycyclic aromatic hydrocarbons in aqueous solutions by a consortium of white-rot fungi. *J. Hazard. Mater.* **2010**, *179*, 845–851.
- (2) Zhu, H.; Aitken, M. D. Surfactant-enhanced desorption and biodegradation of polycyclic aromatic hydrocarbons in contaminated soil. *Environ. Sci. Technol.* **2010**, *44*, 7260–7265.
- (3) Thompson, I. P.; van der Gast, C. J.; Ciric, L.; Singer, A. C. Bioaugmentation for bioremediation: the challenge of strain selection. *Environ. Microbiol.* **2005**, *7*, 909–915.
- (4) García-Junco, M.; De Olmedo, E.; Ortega-Calvo, J. J. Bioavailability of solid and non-aqueous phase liquid (NAPL)-dissolved phenanthrene to the biosurfactant-producing bacterium *Pseudomonas aeruginosa* 19SJ. *Environ. Microbiol.* **2001**, *3*, 561–569.
- (5) Krell, T.; Lical, J. S.; Reyes-Darias, J. A.; Jimenez-Sanchez, C.; Sungthong, R.; Ortega-Calvo, J. J. Bioavailability of pollutants and chemotaxis. *Curr. Opin. Biotechnol.* **2013**, *24*, 451–456.
- (6) Ortega-Calvo, J. J.; Tejada-Agredano, M. C.; Jimenez-Sanchez, C.; Congiu, E.; Sungthong, R.; Niqui-Arroyo, J. L.; Cantos, M. Is it possible to increase bioavailability but not environmental risk of PAHs in bioremediation? *J. Hazard. Mater.* **2013**, *261*, 733–745.
- (7) Tejada-Agredano, M. C.; Gallego, S.; Niqui-Arroyo, J. L.; Vila, J.; Grifoll, M.; Ortega-Calvo, J. J. Effect of interface fertilization on biodegradation of polycyclic aromatic hydrocarbons present in nonaqueous-phase liquids. *Environ. Sci. Technol.* **2011**, *45*, 1074–1081.
- (8) Tejada-Agredano, M. C.; Mayer, P.; Ortega-Calvo, J. J. The effect of humic acids on biodegradation of polycyclic aromatic hydrocarbons depends on the exposure regime. *Environ. Pollut.* **2014**, *184*, 435–442.
- (9) Jimenez-Sanchez, C.; Wick, L. Y.; Ortega-Calvo, J. J. Chemical effectors cause different motile behavior and deposition of bacteria in porous media. *Environ. Sci. Technol.* **2012**, *46*, 6790–6797.
- (10) Furuno, S.; Foss, S.; Wild, E.; Jones, K. C.; Semple, K. T.; Harms, H.; Wick, L. Y. Mycelia promote active transport and spatial dispersion of polycyclic aromatic hydrocarbons. *Environ. Sci. Technol.* **2012**, *46*, 5463–5470.
- (11) Furuno, S.; Pázolt, K.; Rabe, C.; Neu, T. R.; Harms, H.; Wick, L. Y. Fungal mycelia allow chemotactic dispersal of polycyclic aromatic hydrocarbon-degrading bacteria in water-unsaturated systems. *Environ. Microbiol.* **2010**, *12*, 1391–1398.
- (12) Kohlmeier, S.; Smits, T. H.; Ford, R. M.; Keel, C.; Harms, H.; Wick, L. Y. Taking the fungal highway: mobilization of pollutant-degrading bacteria by fungi. *Environ. Sci. Technol.* **2005**, *39*, 4640–4646.
- (13) Wick, L. Y.; Remer, R.; Würz, B.; Reichenbach, J.; Braun, S.; Schäfer, F.; Harms, H. Effect of fungal hyphae on the access of bacteria to phenanthrene in soil. *Environ. Sci. Technol.* **2007**, *41*, 500–505.
- (14) Banitz, T.; Johst, K.; Wick, L. Y.; Schamfuß, S.; Harms, H.; Frank, K. Highways versus pipelines: contributions of two fungal transport mechanisms to efficient bioremediation. *Environ. Microbiol. Rep.* **2013**, *5*, 211–218.
- (15) Harms, H.; Schlosser, D.; Wick, L. Y. Untapped potential: exploiting fungi in bioremediation of hazardous chemicals. *Nat. Rev. Microbiol.* **2011**, *9*, 177–192.
- (16) Sungthong, R.; van West, P.; Cantos, M.; Ortega-Calvo, J. J. Development of eukaryotic zoospores within polycyclic aromatic hydrocarbon (PAH)-polluted environments: A set of behaviors that are relevant for bioremediation. *Sci. Total Environ.* **2015**, *511*, 767–776.
- (17) Sungthong, R.; van West, P.; Heyman, F.; Jensen, D. F.; Ortega-Calvo, J. J. Mobilization of pollutant-degrading bacteria by eukaryotic zoospores. *Environ. Sci. Technol.* **2016**, *50*, 7633–7640.
- (18) Johnsen, A. R.; Karlson, U. Evaluation of bacterial strategies to promote the bioavailability of polycyclic aromatic hydrocarbons. *Appl. Microbiol. Biotechnol.* **2004**, *63*, 452–459.
- (19) Seo, Y.; Lee, W. H.; Sorial, G.; Bishop, P. L. The application of a mulch biofilm barrier for surfactant enhanced polycyclic aromatic hydrocarbon bioremediation. *Environ. Pollut.* **2009**, *157*, 95–101.
- (20) Mangwani, N.; Kumari, S.; Das, S. Involvement of quorum sensing genes in biofilm development and degradation of polycyclic aromatic hydrocarbons by a marine bacterium *Pseudomonas aeruginosa* N6P6. *Appl. Microbiol. Biotechnol.* **2015**, *99*, 10283–10297.
- (21) Niqui-Arroyo, J. L.; Bueno-Montes, M.; Ortega-Calvo, J. J. Biodegradation of anthropogenic organic compounds in natural environments. In *Biophysico-Chemical Processes of Anthropogenic Organic Compounds in Environmental Systems*; Xing, B., Senesi, N., Huang, P. M., Eds.; IUPAC Series on Biophysico-Chemical Processes in Environmental Systems; John Wiley & Sons, Inc.: Hoboken, NJ, 2011; Vol. 3, pp 483–501.
- (22) Vila, J.; Grifoll, M. Actions of *Mycobacterium* sp. API on the saturated- and aromatic-hydrocarbon fractions of fuel oil in a marine medium. *Appl. Environ. Microbiol.* **2009**, *75*, 6232–6239.
- (23) Kostecki, P. T.; Calabrese, E. J. Contaminated soils. In *Diesel fuel contamination*; Lewis Publishers Inc.: Chelsea, MI, 1992.
- (24) Harding, M. W.; Marques, L. L.; Howard, R. J.; Olson, M. E. Can filamentous fungi form biofilms? *Trends Microbiol.* **2009**, *17*, 475–480.
- (25) Grate, J. W.; Dehoff, K. J.; Warner, M. G.; Pittman, J. W.; Wietsma, T. W.; Zhang, C.; Oostrom, M. Correlation of oil–water and air–water contact angles of diverse silanized surfaces and relationship to fluid interfacial tensions. *Langmuir* **2012**, *28*, 7182–7188.
- (26) Lee, H. B.; Kim, B. W. Effect of NAPL exposure on the wettability and two-phase-flow in a single rock fracture. *Hydrol. Process* **2015**, *29*, 4919–4931.
- (27) Fredslund, L.; Sniegowski, K.; Wick, L. Y.; Jacobsen, C. S.; De Mot, R.; Springael, D. Surface motility of polycyclic aromatic hydrocarbon (PAH)-degrading mycobacteria. *Res. Microbiol.* **2008**, *159*, 255–262.
- (28) Gleason, F. H.; Lilje, O.; Marano, A. V.; Sime-Ngando, T.; Sullivan, B. K.; Kirchmair, M.; Neuhauser, S. Ecological functions of zoospore hyperparasites. *Front. Microbiol.* **2014**, *5*, 244.
- (29) Fritzsche, C. Degradation of pyrene at low defined oxygen concentrations by a *Mycobacterium* sp. *Appl. Environ. Microbiol.* **1994**, *60*, 1687–1689.
- (30) Haftka, J. J.; Parsons, J. R.; Govers, H. A.; Ortega-Calvo, J. J. Enhanced kinetics of solid-phase microextraction and biodegradation of polycyclic aromatic hydrocarbons in the presence of dissolved organic matter. *Environ. Toxicol. Chem.* **2008**, *27*, 1526–1532.